

# *In vitro* Degradation and Cytocompatibility of Magnesium-Zinc-Strontium Alloys with Human Embryonic Stem Cells\*

Aaron F. Cipriano, Ren-Guo Guan, Tong Cui, Zhan-Yong Zhao, Salvador Garcia, Ian Johnson, and  
Huinan Liu, *IEEE*

**Abstract** — Magnesium-based alloys have attracted great interest for medical applications due to their unique biodegradable capability and desirable mechanical properties. When considered for medical applications, the degradation rate of these alloys must be tailored so that: (i) it does not exceed the rate at which the degradation products can be excreted from the body, and (ii) it is slow enough so that the load bearing properties of the implant are not jeopardized and do not conflict prior to and during synthesis of new tissue. Implant integration with surrounding cells and tissues and mechanical stability are critical aspects for clinical success. This study investigated Magnesium-Zinc-Strontium (ZSr41) alloy degradation rates and the interaction of the degradation products with human embryonic stem cells (hESC) over a 72 hour period. An *in vitro* hESC model was chosen due to the higher sensitivity of ESCs to known toxicants which allows to potentially detect toxicological effects of new biomaterials at an early stage. Four distinct ZSr41 compositions (0.15 wt.%, 0.5 wt.%, 1 wt.%, and 1.5 wt.% Sr) were designed and produced through metallurgical processing. ZSr41 alloy mechanical properties, degradation, and cytocompatibility were investigated and compared to pure polished Magnesium (Mg). Mechanical properties evaluated included hardness, ultimate tensile strength, and elongation to failure. Degradation was characterized by measuring total weight loss of samples and pH change in the cell culture media. Cytocompatibility was studied by comparing fluorescence and phase contrast images of hESCs after co-culture with Mg alloys. Results indicated that the Mg-Zn-Sr alloy with 0.15 wt.% Sr improved cytocompatibility and provided slower degradation as compared with pure Mg.

## I. INTRODUCTION

Currently, non-degradable metals are widely used for maxillofacial and orthopedic applications; however, their major limitations include stress shielding on surrounding bone, required revision surgeries to remove the implant, and release of harmful wear particulates induced by abrasion [1]. Bioabsorbable polymers are also used for such applications, and while degradable, they often lack the mechanical strength needed for load bearing implants, can lead to implant failure, and produce acidic degradation products that can lead to

tissue inflammation [2, 3]. In an effort to address the limitations associated with current materials, consideration has been given to Magnesium (Mg) based alloys. Advantages of implementing Mg-based alloys as biomaterials include: controllable biodegradability, stable mechanical properties, biocompatibility, and osteoconductivity and osteoinductivity that lead to bone formation [4].

This study focuses on evaluating the effects of alloying Mg with Zinc (Zn) and Strontium (Sr). It has been previously shown that the addition of Sr to Mg and Aluminum alloys improves mechanical properties and surface characteristics as a result of grain refinement [5] and therefore affects both degradation mode and rate. Furthermore, studies have shown that Mg degradation is largely influenced by the composition of surrounding solution which dictates the mode of degradation of the material (e.g. galvanic corrosion, pitting, etc.) [6, 7]. Therefore, in order to simulate physiological conditions, hESC culture media was chosen as the solution in which the degradation studies were conducted [8]. An *in vitro* hESC model was chosen, based on the successful implementation of murine ESC assays [9], to evaluate alloy cytocompatibility due to the higher sensitivity of ESCs to known toxicants which allows for the potential detection of toxicological effects of new biomaterials at an early stage [10]. This research presents a comparative study of the degradation and cytocompatibility of pure polished Magnesium (P-Mg) and four distinct ZSr41 Mg alloys in contact with hESC culture media. P-Mg was included as a standard against which to compare ZSr41. The compositions of ZSr-41 contained between 94.5 wt.% and 95.85 wt.% Mg, 4 wt.% Zn and between 0.15% and 1.5 wt.% Strontium.

## II. MATERIALS AND METHODS

### A. Preparation of Mg and ZSr41 samples

*In vitro* degradation and cytocompatibility studies were performed on four compositionally distinct Mg ZSr41 alloys and P-Mg. The wt.% of Strontium present in each alloy was as follows: 0.15 wt.% Sr for ZSr41A; 0.5 wt.% Sr for ZSr41B; 1.0 wt.% Sr for ZSr41C; and 1.5 wt.% Sr for ZSr41D. These alloys were produced by metallurgical processing. P-Mg (Good Fellow) and ZSr41A, B, C, D samples were all prepared according to the following procedures: first, 5 x 5 mm squares were polished using 600, 800, and 1200 grit silicon carbide abrasive papers (Ted Pella, Inc.) to remove surface oxides. Each sample was subsequently ultrasonically cleaned (VWR, Model 97043-036) for 15 min in 200 proof ethanol (Koptec), individually weighed and disinfected under UV radiation in a

\*Research supported in part by U.S. NSF BRIGE award (CBET 1125801), the University of California, the National Natural Science Foundation of China (Grant 51034002, 50974038 and 51074049), and the Fok Ying Tong Education Foundation (132002).

A. F. Cipriano, I. Johnson, and H. Liu are affiliated with the Department of Bioengineering, University of California, Riverside CA 92521 USA. R.-G. Guan, T. Cui, and Z.-Y. Zhao are affiliated with Northeastern University, Shenyang, China. S. Garcia is affiliated with California State University, San Bernardino, (Corresponding author H. Liu, phone: 951-827-2944, fax: 951-827-6416, email: [huinan.liu@ucr.edu](mailto:huinan.liu@ucr.edu))

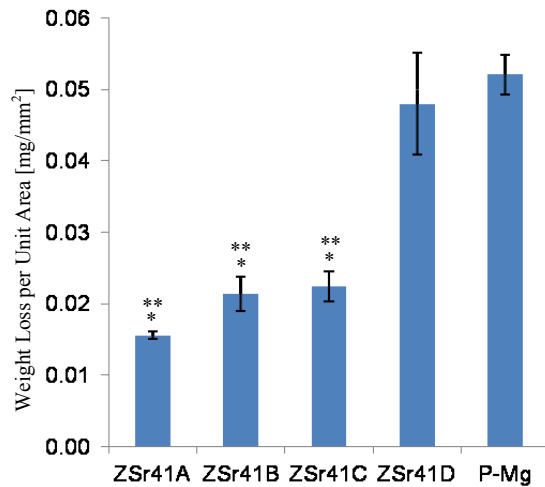


FIGURE 1 Total weight loss per unit area of ZSr41 alloys and the control after culturing with H9 hESC for 72 hours. Values are mean  $\pm$  SEM; n = 3; \* $p$ <0.05 compared to ZSr41D; \*\* $p$ <0.05 compared to P-Mg.

class II biosafety cabinet for 4 hours on each side prior to degradation and cell culture experiments.

**Material Characterization:** A microcomputer controlled electronic universal mechanical testing machine (CMT5105) was used to determine hardness, ultimate tensile strength (UTS), and elongation to failure.

#### B. H9 human embryonic stem cell culture

In order to monitor stem cell differentiation, H9 human embryonic stem cells (H9-hESCs) were stably transfected with green fluorescence protein (GFP) at the octamer-binding transcription factor 4 (OCT4) promoter site using Gene Juice (Novagen), knockout Dulbecco's modified eagle's medium (KO-DMEM/F12; Invitrogen) and plasmid pCAG-eGFP-Internal Ribosome entry site (IRES)-Puromycin-R. Feeder-free conditions in a T-25 flask (Falcon) with Geltrex<sup>TM</sup> matrix (Invitrogen) and mTeSR@1 media (STEMCELL Technologies) were used to maintain H9-OCT4 hESCs. Finally, H9-OCT4 hESCs were passaged using Accutase (Innovative Cell Technologies) and glass beads upon light microscope verification of 80-90% confluency.

**Initial stem cell characterization:** Morphology and fluorescence of H9-OCT4 hESCs were observed using the Nikon Eclipse Ti microscope. Morphology was determined using phase contrast images. Fluorescent images were used to identify undifferentiated stem cells.

#### C. Culturing of H9-OCT4 hESC with ZSr41 alloys

The immersion method was used to investigate P-Mg and ZSr41 degradation. Two 12-well plates (BD Falcon) were prepared by covering 18 wells with cold Geltrex<sup>TM</sup> matrix (Invitrogen) in DMEM media (Invitrogen 11965092) (1:50) for 24 hours. The excess Geltrex<sup>TM</sup> solution was aspirated and H9-OCT4 ESCs were seeded (passage 15) onto the wells with mTeSR@1 media and maintained for 24 hours under standard cell culture conditions (37°C, 5% CO<sub>2</sub>). Details of the composition of the commercially available mTeSR@1

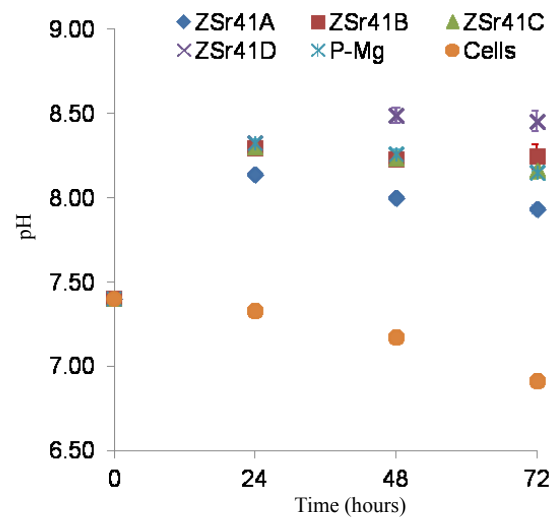


FIGURE 2 Change in pH of H9 hESC culture media as a result of degradation of ZSr41 alloys, P-Mg, and blank control (cells only). Values are mean  $\pm$  SEM; n = 3;  $p$ <0.05 when comparing ZSr41A to other ZSr41 compositions, P-Mg, and blank control at all time points.

hESC culture feeding media used are described elsewhere [11].

After the initial 24 hour incubation period, the mTeSR@1 media was removed and replenished with fresh solution. Then Mg and ZSr41A, B, C and D samples were placed in trans-well inserts (Corning) and positioned within the wells where H9-OCT4 ESCs were cultured. Blank control for cytocompatibility consisted of mTeSR@1 media with H9-OCT4 ESC only. Cell culture was continued and moved to the Nikon Biostation CT where incubation was carried under standard conditions in order to monitor degradation and cytocompatibility over time.

#### D. In Vitro degradation of ZSr41 alloys

Following preparation, the samples were incubated for a total of 72 hours. Incubation intervals were set at every 24 hours to mimic *in vivo* conditions where the circulatory system regularly removes soluble degradation products from the local implantation site. At each prescribed incubation interval, the culture media was collected and removed to measure pH levels and subsequently replaced with new culture media under sterile conditions. Caution was taken in order to avoid disrupting degradation products on the specimen surface while removing the culture media along with any soluble degradation products found within. Measurements for pH levels were done using a calibrated pH meter (VWR, Model SB70P) and values were used to quantify pH changes with respect to incubation time. At the end of the total incubation period, each sample was individually weighed and values were used to calculate the percent mass loss with respect to incubation time.

#### E. In Vitro cytocompatibility of ZSr41 alloys with hESC

Phase contrast and fluorescence (Nikon Biostation CT) images of two random points of each well were captured at 6 hour intervals throughout the total incubation period to capture cell viability in response to Mg and ZSr41 degradation products. The area of viable cells in images showing positive OCT4 stem cell marker were outlined manually in ImageJ software in order to quantify viable cell

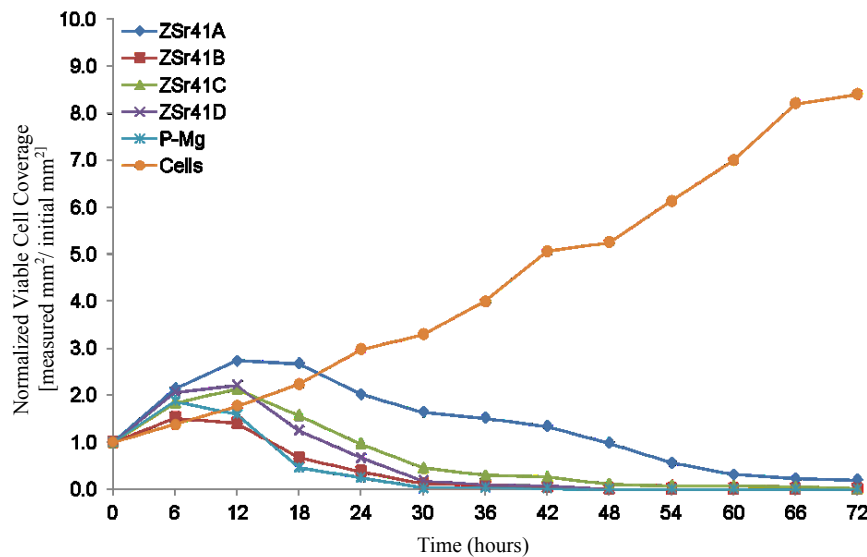


FIGURE 3 The change of viable H9 hESC coverage over time after exposure to ZSr41 alloys and P-Mg degradation products as compared with the blank control (cells only). The viable cell coverage area at each time point was normalized by the initial cell coverage area at time zero.

coverage. These values of viable cell area coverage were used to calculate a normalized value of cell coverage area of H9-OCT4 hESCs over time.

#### F. Statistical Analysis

In vitro degradation and cytocompatibility experiments were run in triplicate. Numerical data sets were analyzed using standard analysis of variance (ANOVA) followed by standard post hoc tests with the Holm-Bonferroni correction; statistical significance was considered at  $p < 0.05$ .

### III. RESULTS

#### A. Mechanical Properties of ZSr41 alloys

The hardness of Mg-4wt%Zn-1wt%Sr was measured to be 71.5 HV, while the ultimate tensile strength and elongation to failure were measured at 270 MPa and 12.8% respectively. Compared to published values for P-Mg, UTS of 160 MPa and 3-15% elongation [12], the UTS of Mg-4wt%Zn-1wt%Sr was improved by a factor of nearly 1.7.

#### B. In Vitro degradation of ZSr41 alloys

Results from the 72 hour immersion study indicated that total weight loss per unit area was significantly lower for ZSr41A, B, and C when compared to ZSr41D and P-Mg (Figure 1). Further weight loss analysis revealed that ZSr41B and ZSr41C exhibited similar behavior, while ZSr41D showed the highest weight loss from the samples studied. When compared to the behavior of P-Mg, overall, ZSr41A, B, C, and D showed less weight loss.

Analysis of the pH change data showed that ZSr41A had a significantly lower effect on pH increase when compared to the other alloy compositions and P-Mg throughout all time intervals (Figure 2). Results also indicated a similar pH change trend for ZSr41B, ZSr41C, and P-Mg during all time intervals as a result of their degradation products. The pH change measured for ZSr41D was the highest of all the alloys and P-Mg tested. Comparison between the change in pH from the alloy and P-Mg samples to the blank control (cells only)

revealed that degradation products from all samples caused an increase in pH, while the blank control caused a decrease in pH.

Taken together, both weight loss and pH change results allowed ranking of the samples, starting from slowest degradation, as follows: ZSr41A < ZSr41B ~ ZSr41C < ZSr41D ~ P-Mg.

#### C. In Vitro Cytocompatibility of ZSr41 alloys with hESC

Fluorescence images from the 72 hour cell culture study showed improved H9 hESC cytocompatibility with ZSr41 alloys compared to P-Mg, of which, ZSr41A showed best cytocompatibility overall. Cell viability curves were calculated from fluorescence and phase contrast images, and results are plotted in Figure 3. In contrast to P-Mg where viable cells were no longer visible at 30 hours of culture, all of the ZSr41 alloys still exhibited coverage of viable cells. Results from both ZSr41B and ZSr41D indicated similar cell response towards these alloys, where lack of viable cells was observed at 48 hours of culture. Furthermore, ZSr41C alloy showed an improved cell response, compared to ZSr41B and D, where cell viability was visible almost near the end of the 72 hour study. Only results from alloy ZSr41A showed cell viability at the end of the study (Figure 4). All samples exhibited an initial increase in cell coverage followed by a steady decrease over time. During this the initial interval (0-14 h) cells lose their closely packed organization and begin to disperse. In contrast to the blank control with cells only, all alloy and P-Mg samples showed a decrease in percentage of cell coverage. Cell viability results allow ranking of the alloy and P-Mg samples, starting from most cytocompatible, as follows: ZSr41A > ZSr41C > ZSr41B ~ ZSr41D > P-Mg.

### IV. DISCUSSION

In this study, ZSr41 alloys were immersed in hESC culture media in order to mimic a physiological environment where cell-implant interaction can be studied. The results provided evidence of how fast these Mg alloys degrade in physiologically simulated conditions, and how cells responded to degradation products. *In vitro* H9 hESC culture



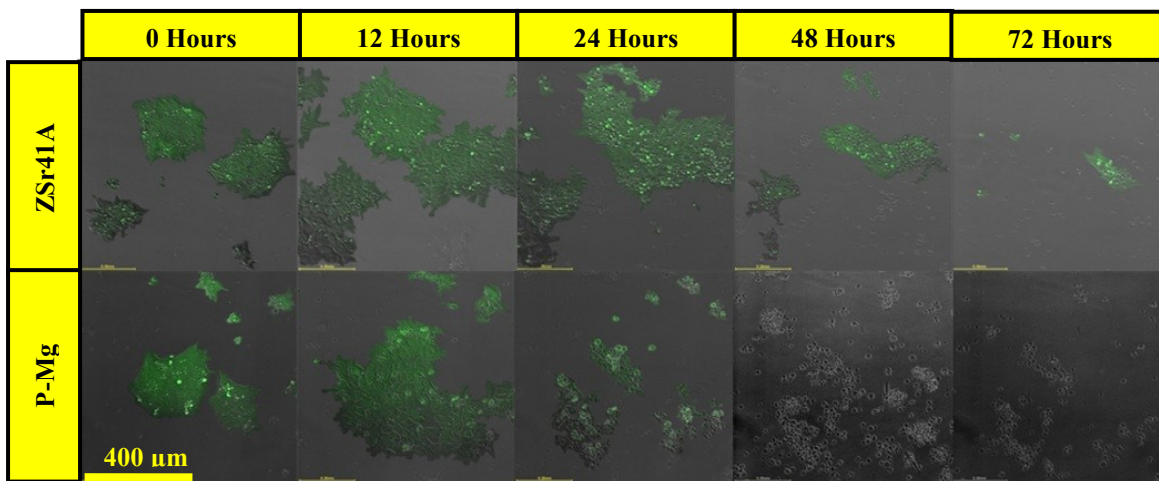


FIGURE 4 Montage of merged fluorescence and phase contrast images of H9 hESCs when co-cultured with ZSr41A and P-Mg at the prescribed time intervals during the 72 h of cell culture. All images in the montage have the same magnification as shown by the 400  $\mu\text{m}$  scale bar.

results suggested that ZSr41A alloy exhibited superior cytocompatibility as compared with ZSr41B, C, D, and P-Mg. This superior cell response can be attributed to less pronounced effect of ZSr41A on pH increase of hESC culture media as compared with the other materials studied.

The pH increase is attributed to the Mg degradation mechanism and formation of products as described by the following equations:



Equation 1 indicates the formation of an Mg oxidation layer which is in turn attacked by chlorine ions (Equation 2) to form a  $\text{MgCl}_2$  (depending on the solubility of the salt in the cell culture media) and hydroxide ions ( $\text{OH}^-$ ). An increase in concentration of hydroxide ions is proportional to the observed increase in pH. Thus, improved degradation resistance leads to lower hydroxide ion production and a lower increase in pH. The weight loss results confirmed a slower degradation of ZSr41A which in turn contributed to the lower increase in pH discussed above.

## V. CONCLUSION

Results indicated improvement in ZSr41 alloy mechanical properties compared to P-Mg. Results also showed enhanced cytocompatibility with the ZSr41A alloy compared to the other studied compositions of ZSr41. Enhanced cell viability observed with ZSr41A was a result from lower pH increase in hESC culture media and slower rate of mass loss indicative of slower degradation. In this study we utilized H9 hESCs due to the inherent sensitivity and the potential to serve as a clinically relevant *in vitro* model to demonstrate biocompatibility and safety of novel biomaterials. As a result from this *in vitro* study, Mg ZSr41A shows potential as a biomaterial for orthopedic and maxillofacial implant applications.

## VI. FUTURE WORK

In order to further understand and elucidate the relationship between ZSr41 degradation and cytocompatibility, it is necessary to explore the role of

surface features and composition before and after cell culture. In addition, electrochemical tests are also required in order to elucidate corrosion behavior and how it correlates with the addition of the alloying elements. Continued *in vitro* studies will help identify optimal alloy composition for future *in vivo* evaluation.

## ACKNOWLEDGMENTS

The authors would like to thank the U.S. NSF BRIGE award (CBET 1125801), the University of California, National Natural Science Foundation of China (grant 51034002, 50974038 and 51074049) and the Fok Ying Tong Education Foundation (132002) for financial support.

## REFERENCES

- [1] D. J. Breen and D. J. Stoker, "Titanium lines: A manifestation of metallosis and tissue response to titanium alloy megaprotheses at the knee," *Clinical Radiology*, vol. 47, pp. 274-277, 1993.
- [2] N. Tran and T. J. Webster, "Nanotechnology for bone materials," *Wiley Interdiscip Rev Nanomed Nanobiotechnol*, vol. 1, pp. 336-51, May-Jun 2009.
- [3] D. J. Beevers, "Metal vs bioabsorbable interference screws: initial fixation," *Proc Inst Mech Eng H*, vol. 217, pp. 59-75, 2003.
- [4] I. Johnson, *et al.*, "In vitro evaluation of the surface effects on magnesium-yttrium alloy degradation and mesenchymal stem cell adhesion," *J Biomed Mater Res A*, Nov 29 2011.
- [5] H. Borkar, *et al.*, "Effect of strontium on flow behavior and texture evolution during the hot deformation of Mg-1&#xa0;wt%Mn alloy," *Materials Science and Engineering: A*, vol. 537, pp. 49-57, 2012.
- [6] Y. Xin, *et al.*, "Influence of aggressive ions on the degradation behavior of biomedical magnesium alloy in physiological environment," *Acta Biomater*, vol. 4, pp. 2008-15, Nov 2008.
- [7] R. Rettig and S. Virtanen, "Composition of corrosion layers on a magnesium rare-earth alloy in simulated body fluids," *J Biomed Mater Res A*, vol. 88, pp. 359-69, Feb 2009.
- [8] N. I. Zainal Abidin, *et al.*, "Corrosion of high purity Mg, AZ91, ZE41 and Mg2Zn0.2Mn in Hank's solution at room temperature," *Corrosion Science*, vol. 53, pp. 862-872, 2011.
- [9] A. E. Seiler and H. Spielmann, "The validated embryonic stem cell test to predict embryotoxicity in vitro," *Nat Protoc*, vol. 6, pp. 961-78, Jul 2011.
- [10] G. Laschinski, *et al.*, "Cytotoxicity test using blastocyst-derived euploid embryonal stem cells: A new approach to in vitro teratogenesis screening," *Reproductive Toxicology*, vol. 5, pp. 57-64, 1991.
- [11] T. E. Ludwig, *et al.*, "Feeder-independent culture of human embryonic stem cells," *Nat Methods*, vol. 3, pp. 637-46, Aug 2006.
- [12] D. R. Askeland and P. P. Fulay, *Essentials of materials science and engineering*. Australia: Thomson, 2004.